

## VENTILATION OF DOUBLE FAÇADES

Dipl.-Ing. M.Sc.(dist) Jörn von Grabe<sup>1,2</sup>

Dipl.-Phys. Rüdiger Lorenz<sup>2</sup>

Dr. Ben Croxford<sup>1</sup>

<sup>1</sup>Bartlett Graduate School, UCL,  
Gower Street, London,  
United Kingdom, WC1E 6BT  
b.croxford@ucl.ac.uk

<sup>2</sup>Michael Lange, Beratender Ingenieur  
Wilmsdorfer Str. 145-146,  
10585 Berlin,  
J.v.Grabe@t-online.de

### ABSTRACT

This paper deals with the development and the testing of a simulation algorithm for the temperature behaviour and the flow characteristics of double façades. It has been developed in order to obtain a tool which enables the energy consultant to make quick design decisions without being required to use fairly complicated CFD tools.

In order to determine the degree of accuracy of the algorithm, a double façade has been monitored under controlled conditions and the results have been compared against the predicted values for several design situations. The resulting inaccuracy in some cases can be traced back to how the flow resistance of various geometries are modelled.

### INTRODUCTION

The paper starts with an explanation of the assumptions made for the development of the algorithm. These are related to simplifications concerning the geometric model including heat flows and the flow direction. In a first step the temperature function and the flow function are developed separately. Starting from fundamental and established functions (energy transport equation, Bernoulli) due to space reasons only the basic steps of the development not the complete calculations including transformations can be outlined. Finally it is explained how these equations have to be combined to obtain the complete method.

Characteristic results of the monitoring are presented subsequently, followed by a brief discussion of the main reasons for any inaccuracy.

### MODEL

Some assumptions made in the course of this work concern the relevant input parameters and the necessary output. These assumptions are based on our experience as consulting engineers and are summarised here:

To be useful the simulation of a double façade must yield information about

- the air mass flow through the façade gap to control the possibility of natural ventilation of the room behind,
- the temperature of the façade air related to the height of the façade which determines the temperature of the supply air in the case of natural ventilation. It also helps in estimating the cooling load required in the case of conditioning,
- the temperature of the façade perimeter to predict possible deformations of the materials due to thermal elongation.

Design parameters which have the main influence on the air mass flow and the temperatures are the following:

- the size of the upper and the lower vent of the façade,
- the depth of the façade and the position of the shading device in the depth of the façade gap,
- the material of the shading device, especially the absorption coefficient,
- the size of the vents of the shading device,
- the quality of the outer and the inner pane, especially the solar transmission factor but also the U-value and the absorption coefficient.

Consequently, these parameters are included in the temperature and the flow algorithm.

There are different types of double façades, however, usually all types have constructional parameters in common which have been extracted and simplified. This process is demonstrated in figure (A1). The most important simplification is the fact, that the air exchange between façade gap and the room behind is not included in the algorithm. We consider this as the design case since the air temperature must be determined for the moment when the room window is first opened by the occupant.

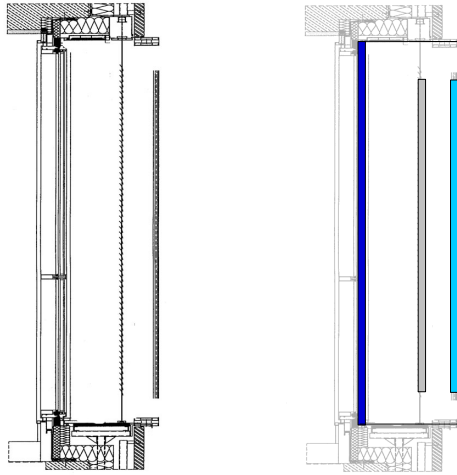


Fig.(A1):

Applied simplification of the double façade geometry

For a better understanding of the terms used for the geometry, the model is shown in figure (A2). With those terms it is important to note, that shaft 1 is always the shaft between shading device and external climate and shaft 2 is the shaft between shading device and internal climate. This is also true for the monitoring results, even though the façade is then ventilated with air of the internal climate.

Further on, the determination of the direction of the different heat flows is part of the development of the algorithm. This accounts for some further assumptions. Firstly the flow is assumed to be reduced to one dimension (later a second dimension is introduced by separating the flow behind and in front of the shading device). Thus, the air mass flow is one directional in either the positive or negative y direction.

The temperature function works with a net mass flow in the y direction through the system so that there is no consideration of local, secondary, reverse currents. This will however, be taken into account by modelling the flow resistance.

There is also no consideration of any diagonal flow, in y-z direction for example.

The molecular heat transport is assumed to be normal to the air flow, in a positive or negative x direction.

Transient effects are not considered.

## TEMPERATURE FUNCTION

The temperature function  $T_s(y)$  for the shaft air over the height of the system H is generally based on the energy transport equation (t1).

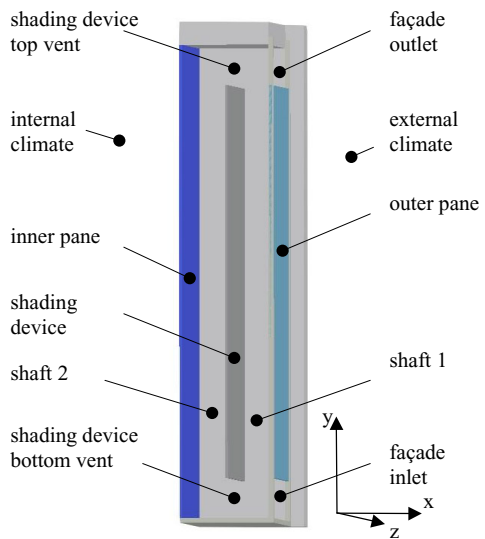
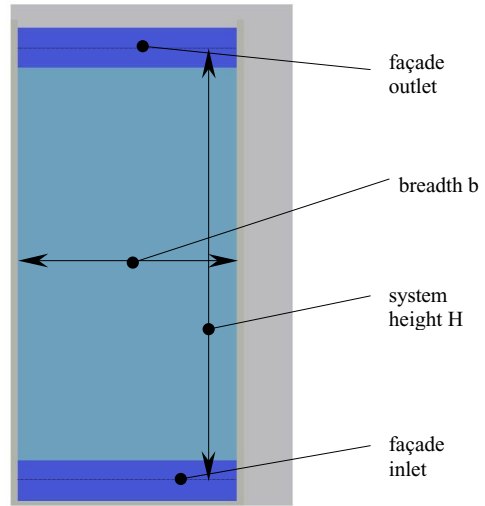


Fig.(A2):

Geometric model of the façade system with designation of the elements and domains.

(t1)

$$\rho * c * \frac{\partial T}{\partial t} + (\rho * \mathbf{w}) * c * \text{grad } T = k * \text{div grad } T + \tilde{q}$$

Only steady state conditions are considered and single heat sources do not occur. The function reduces to:

$$(\rho * \mathbf{w}) * c * \text{grad } T = k * \text{div grad } T$$

The molecular heat transport within the air (right side of the equation above) is not considered, only the net heat flow into and out of the gap in a positive or negative x-direction. Moreover, the convective transport is taken as the net heat flow in the main direction y. Therefore:

$$(\rho * w_y) * c * \frac{dT_s}{dy} = \frac{h_c}{d} * (T_p(y) - T_s(y))$$

Or with the mass flow density  $\hat{m} = \rho * w$

(t2)

$$\hat{m} * c * d * dT_s(y) = h_c * (T_P(y) - T_s(y)) * dy$$

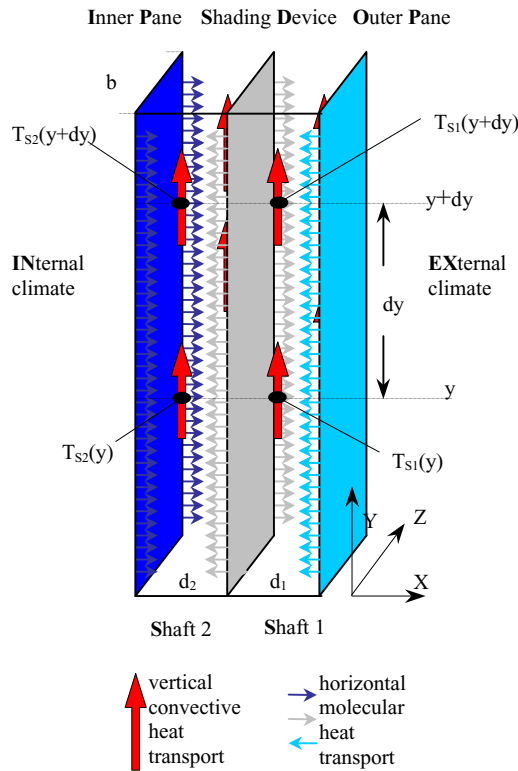


Fig. (T1):

Schematic representation of the directions of the heat flow as assumed for the simulation. Relate this to equation (t2).

For the shafts, the convective heat transfer coefficient may differ due to different air temperatures and air velocities within the shafts. Therefore for both shafts the convective heat transfer coefficient is treated separately. For the calculation, the approach of Michejew (see Elsner) has been used which has been developed for free convection at vertical planes. According to this approach the heat transfer only depends on the Rayleigh number which is determined by a number of parameters including thermal diffusivity, temperature difference, and height of the surface. The calculation results in a mean heat transfer coefficient over the height of the system  $h_{c,m,S}$ .

Since greatly different surface temperatures may occur, the radiative heat exchange between the surfaces (e.g i and j) must not be neglected. It is approximated by the radiative heat exchange factor, valid for two parallel planes with infinite expansion and is also averaged over the height of the system:

$$h_{r,m} = \frac{C_{i-j}}{100^4} * [(T_{m,i} + T_{m,j})^3 - 2 * (T_{m,i} + T_{m,j}) * T_{m,i} * T_{m,j}]$$

The factor  $C_{i-j}$  includes the Stefan-Boltzmann constant and the grey body view factors.

For the heat exchange between the system and the ambient climate, the standard exchange factors as found in CIBSE (Guide A3) are used.

The driving force is the sun's radiation that is absorbed by the surfaces of the double facade. These surfaces are mainly the shading device (SD), the inner pane (IP) and the outer pane (OP). The absorbed energy, determined by the solar intensity and the absorption coefficient of the material, leads to an energy flow to and from the element to its surrounding (either shaft air by convection, the other planes by radiation or to the external/ internal climate by both). The absorbed solar energy  $\hat{q}$  must equal the total of the element's heat flow. It is shown as example for the outer pane:

$$\begin{aligned} \hat{q}_{OP} = & (T_{OP}(y) - T_{EX}) * h_{OP-EX} + \dots \\ & (T_{OP}(y) - T_{S1}(y)) * h_{c,m,S1} + \dots \\ & (T_{OP}(y) - T_{SD}(y)) * h_{r,m,SD-OP} \end{aligned}$$

The equation can be transformed to obtain the temperature function for the surface:

$$T_{OP}(y) = \frac{\hat{q}_{OP} + T_{EX} * h_{OP-EX} + T_{S1}(y) * h_{c,m,S1} + T_{SD}(y) * h_{r,m,SD-OP}}{\sum h_{OP}}$$

Doing this for all three surfaces, a set of equations for all surface temperatures is obtained, each depending at least on one of the shaft air temperatures, another surface temperature or the external/ internal climate.

It is now necessary to eliminate every unknown of the equation except for the air temperature. This can be done e.g. by inserting the  $T_{OP}$ -function and the  $T_{IP}$ -function into the  $T_{SD}$ -function, leaving only the  $T_{S1}$ -function as unknown. Finally, we are left with a system of functions.

(t3)

$$\begin{aligned} T_{OP}(y) = & T_{S1}(y) * h_{c,m,S1} * Z_{OP1} + \dots \\ & T_{S2}(y) * h_{c,m,S2} * Z_{OP2} + G_{OP} \end{aligned}$$

$$\begin{aligned} T_{IP}(y) = & T_{S1}(y) * h_{c,m,S1} * Z_{IP1} + \dots \\ & T_{S2}(y) * h_{c,m,S2} * Z_{IP2} + G_{IP} \end{aligned}$$

$$\begin{aligned} T_{SD}(y) = & T_{S1}(y) * h_{c,m,S1} * Z_{SD1} + \dots \\ & T_{S2}(y) * h_{c,m,S2} * Z_{SD2} + G_{SD} \end{aligned}$$

In equation (t3) the abbreviation Z consist of multiples and sums of the different heat transfer coefficients related to the respective shaft air temperature. It gives valuable information about the ratio of the different heat flows and with that about there influence on the surface temperature.

Moreover it can be seen that the temperatures of the surfaces are determined by both, the shaft air temperatures and a constant G. This summand is determined by the constant solar energy and the temperature of the internal and the external climate.

Each of these equations can now be inserted into (t2) whereas shaft 1 (see figure (T1)) gets energy from the outer pane (OP) and the shading device (SD) and shaft 2 gets energy from the inner pane (IP) and the shading device.

Transformation yields a two dimensional system of first order linear differential equations:

$$T'_{s1}(y) = T_{s1}(y) * a_{11} + T_{s2}(y) * a_{12} + g_1$$

$$T'_{s2}(y) = T_{s1}(y) * a_{21} + T_{s2}(y) * a_{22} + g_2$$

or, writing with vectors and matrices:

$$\mathbf{T}'(y) = \mathbf{A} * \mathbf{T}(y) + \mathbf{g}$$

The abbreviations a and g, again consist of multiples of the heat transfer coefficients and the solar intensity/climate. These are not analysed here for space reasons.

The system can be solved in two steps. Firstly the homogeneous solution must be found by calculating the Eigenvalues and Eigenvectors and secondly the non-homogeneous solution must be determined. For the latter, the method of undetermined coefficients can be used.

The Eigenvalue problem leads to an exponential function whereas the non-homogeneous solution yields an additional constant part. The temperature functions are:

(t4)

$$T_{s1}(y) = IC_1 * x^{(1)} * e^{\lambda_1 * y} + IC_2 * x^{(2)} * e^{\lambda_2 * y} + u_1$$

$$T_{s2}(y) = IC_1 * e^{\lambda_1 * y} + IC_2 * e^{\lambda_2 * y} + u_2$$

With these equations the scalar value IC is another unknown which must be determined with help of the initial conditions. These are given as the air temperatures at the point  $y = 0$ , the starting temperature  $T_{start}$ . It may chosen as an arbitrary value but will normally be the external temperature since the façade gap is ventilated with external air.  $x^{(i)}$  are the Eigenvectors and  $\lambda$  the Eigenvalues of the system. The letter u is a constant which describes the air temperature within the shafts when no further heat exchange takes place (for  $y = \infty$ , the Eigenvalues are always negative).

As described above, the determination of the heat exchange coefficients requires the mean temperature of the air and of the surfaces over the height of the

system. They can easily be determined from equation (t4) by integration.

## FLUID DYNAMICS

For the motion of the air, only buoyancy forces are taken into account. There may also be wind pressure as a driving force, but firstly, wind pressure is extremely unpredictable and secondly, lack of wind pressure normally is the design case.

The starting point is the Bernoulli equation (f1):

(f1)

$$\frac{p_1}{\rho} + \frac{w_1^2}{2} + g * y_1 = \frac{p_2}{\rho} + \frac{w_2^2}{2} + g * y_2 + e_{diss,1-2}$$

It says, that the sum of energy per mass [Nm/kg] remains the same between point 1 and point 2 of a streamline and may only change its character between static, dynamic, potential and dissipated energy. Strictly speaking, the Bernoulli equation is only applicable for systems with constant density  $\rho$  (what is not the case here). However, if a system is divided into a number of finite subsystems and the fluid properties are regarded as constant for each subsystem, the pressure  $p_i$  might be related to the respective density  $\rho_i$ .

For the simulation, only two subsystems have been chosen (see figure (F1)): the external air (state 1) and the façade air (state 2). Air mass has to be accelerated from zero external velocity ( $w_1 = 0$ ) to a mean velocity within the shaft of  $w_2 = w_{m,S}$ .

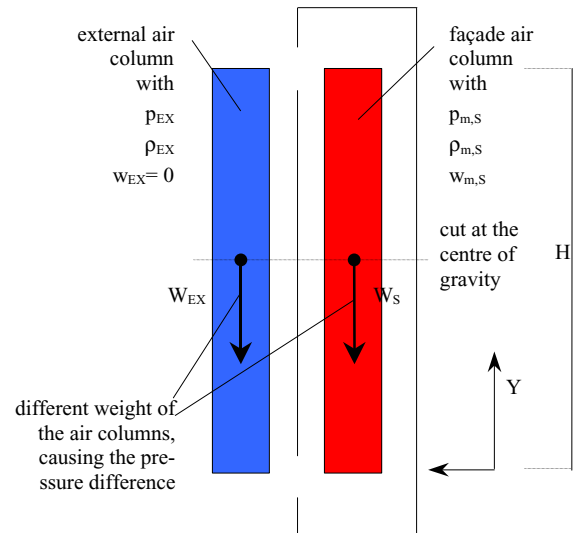


Fig. (F1): Schematic representation of the inner air column (inside the façade: red/dark) and the external air column (outside the façade: blue/light).

The system has to be cut at the centre of gravity of each subsystem. For both it is taken at  $H/2$ . However

this is not completely true for the façade air (the density function is an exponential function as well as the temperature function) but is regarded as a minor simplification (see figure (F1)). Thus, the potential energy can be cancelled out.

With new abbreviations, Bernoulli is now:

$$\frac{p_{EX}}{\rho_{EX}} = \frac{p_{m,S}}{\rho_{m,S}} + \frac{w_{m,S}^2}{2} + e_{diss,1-2}$$

Here we consider only the pressure difference  $\Delta p$  between inside and outside. Static equilibrium yields:

$$\Delta p = (\rho_{m,S} - \rho_{EX}) * g * H$$

With a chosen reference level for the external pressure  $p_{EX} = 0$ , the equation for the shaft air velocity becomes:

(f2)

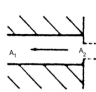
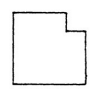

$$w_{m,S} = \sqrt{2 * \left( \frac{(\rho_{EX} - \rho_{m,S}) * g * H - e_{diss,1-2}}{\rho_{m,S}} \right)}$$

With buoyancy driven natural ventilation it is a very common thing, to determine the dissipated energy in a similar way to the determination of the turbulence losses of pipes. They are normally expressed as a multiple ( $\zeta_i$ ) of the square of the local velocity  $w_i$ . The frictional losses play a minor role but might be added; they are analytically derived from a parabolic, symmetrical velocity profile (Hagen-Poiseuille-Flow) for pipe flow. Basically, the losses are:

(f3)

$$e_{diss,1-2} = \sum_i \zeta_i * \frac{w_i^2}{2}$$

The method of interpreting the type of loss to be used is important and here is considered as follows:

Kind	Geometry	Where
inlet and outlet orifice		For the vents at the top and the bottom of the façade
bends		For any redirection of the flow
duct branch and duct union		For the separation of the flow into shaft 1 and shaft 2 at the bottom of the shading device and the union at the top of the shading device

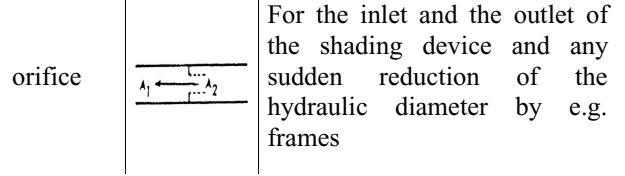


Fig.(F2): Summary of most important single resistance geometries.

Alternatively to modelling orifices for inlet and outlets, flanges and diffusers might be appropriate. Values for  $\zeta$  can be found e.g. in CIBSE guide C4. It is important to mention, that for any required area ratio, the hydraulic ratio has to be taken not the geometric ratio.

The velocity  $w_i$  at the single resistance is determined by the continuity equation. No mass sources or sinks occur, therefore:

$$\rho_{m,S} * w_{m,S} * A_S = \rho_{i,S} * w_{i,S} * A_{i,S} = \dot{m}_S = \text{constant}$$

(f4)

$$w_{i,S} = w_{m,S} * \frac{\rho_{m,S}}{\rho_{i,S}} * \frac{A_S}{A_{i,S}}$$

This is the local velocity expressed as a multiple of the mean velocity of the shaft.  $A_S$ , the cross sectional area of the shaft, is regarded to be constant in this context. The only exception is of course the local reduction or enlargement to  $A_{i,S}$  at the local resistance.

Equation (f4) is important for determining the velocity at a resistance that belongs to only one shaft, either shaft 1 or shaft 2. With inlet and outlet and “duct branch” and “duct union” however, both shafts have to be considered. For inlets and outlets, the velocity not at the orifice but at a point within the undisturbed shaft is needed. Therefore a “virtual shaft velocity”,  $w_{virt,S}$ , has to be determined, again based on the continuity equation. It says that the total mass flowing through the double façade system consists of the sum of the masses flowing through each of the shafts.

$$\dot{m}_S = \dot{m}_{S1} + \dot{m}_{S2}$$

leading to

$$\rho_S * w_{virt,S} * (A_{S1} + A_{S2}) = \rho_{m,S1} * w_{m,S1} * A_{S1} \dots + \rho_{m,S2} * w_{m,S2} * A_{S2}$$

and finally leading to (for shaft 1)

(f5)

$$w_{virt,S} = w_{m,S1} * \frac{\rho_{m,S1} * A_{S1} + \rho_{m,S2} * \frac{w_{m,S2}}{w_{m,S1}} * A_{S2}}{\rho_S * (A_{S1} + A_{S2})}$$

and a similar equation for shaft 2. It is again an expression of the “local” velocity as a multiple of the mean air velocity.

Equations (f4) and (f5) both contain the density  $\rho$  of the air. Simplifying, the ideal gas law can be used to determine it.

$$\rho = \frac{P}{R_{air} * T}$$

If the mean density over the height of the system  $\rho_{m,S}$  is to be taken, the mean air temperature obtained from equation (t4) (after integration) can be used. For the inlet resistance and the “duct branch”, the density of the external air  $\rho_{EX}$  can be used, whereas for the “duct union” and the outlet resistance the density must be determined from the temperature and the mass flows of the two shafts,  $T_{S1,top}$ ,  $T_{S2,top}$  and  $m_{S1}$ ,  $m_{S2}$ .

The loss values  $\zeta$  now turn into  $\zeta_{effective}$ . E.g., equation (f3) can, in combination with (f4), be rewritten as

$$e_{diss,1-2} = \frac{w_{m,S}^2}{2} * \sum_i \zeta_i * \left( \frac{\delta_{m,S} * A_S}{\delta_{i,S} * A_{i,S}} \right)^2$$

or

$$e_{diss,1-2} = \frac{w_{m,S}^2}{2} * \sum_i \zeta_{i,effective}$$

$\sum_i \zeta_{i,effective}$  must be completed by adding the respective factors of (f5) so that the final equation for the mean shaft air velocity of shaft 1 becomes

(f6)

$$w_{m,S1} = \sqrt{\frac{2 * (\rho_{EX} - \rho_{m,S1}) * g * H}{\rho_{m,S1} * \left( 1 + \sum_i \zeta_{i,effective,S1} \right)}}$$

and similarly for shaft 2 (by changing the index S1 to S2).

Comparing this with the derivation of the temperature function it becomes clear, that the temperature distribution over the height of the double façade is dependent on the mass flow through it. On the other hand, the air velocity is dependent on the density of the air, which is determined by the temperature of the air. Consequently, the problem has to be solved by an iteration process. It can be started with an arbitrary value for the mass flow and sensible values for the heat transfer coefficients. With (f6) the resulting mass flow density  $\hat{m} = w_{m,S} * \rho_{m,S}$  caused by the buoyancy can be calculated and used as an improved value for the temperature function. Within the same step, the heat transfer coefficients should be

newly determined. The solution might converge after less than ten steps (depending on the accuracy requirements).

## MONITORING

In order to test the developed algorithm, a purpose built double façade had been monitored over a period of time. The experimental set up had the required geometric variability (to change vent sizes and so on) and had been "turned" around. This means, even though it was part of the building façade it was closed to the external climate and opened to the internal climate. Thus, it was still fully exposed to the external temperature and the solar radiation but ventilated with internal air (which does not affect the testing of the algorithm). This also avoided the effect of wind pressure on the ventilation of the façade.

The incident solar radiation on the shading device (not on the external pane!) has been measured using a Pyranometer (CM11, WMO secondary standard), the air velocity was measured at about the mid-point of the façade height using four anemometers and the air and surface temperatures had been measured at three heights using thermocouples. The total height of the façade was 2.05 m, the breadth 0.95 m and the total depth (both shafts) was 0.24 m.

Two characteristic monitoring results shall be discussed here. With the help of these the attention shall be directed to the sensitive dependence of the prediction on the modelling of the flow resistance, especially the resistance of inlet and outlet geometry.

The excerpt presented here shows the air temperature at the top of the shafts. It is presented as percentage increase of internal air temperature over incident solar radiation. Thus, the influence of the external air temperature has been neglected for the presentation. This is justifiable as long as the external temperature is constant over the monitoring period (which was the case). The prediction has both an upper and a lower limit. This was calculated according to the accuracy of the monitoring equipment. However this is not presented here as it has only little meaning in this context.

The set up for Measurement 1 was with the shading device placed at the midpoint of the shaft depth (0.12 m), an inlet and outlet height of 0.04 m, a shading device inlet height of 0.17 m and a shading device outlet height of 0.17 m as well.

The best of the two prediction lines (figure (M1)) was achieved by modelling both the inlet and outlet as a flange with an abrupt enlargement to the duct diameter and a diffuser with a preceding abrupt contraction. For both shafts there is only a small deviation between monitored and modelled. The upper prediction line ("prediction 2") shows the

results of the modelling of the inlet and outlet as orifices. Here there is a factor of 2 difference between measurement and prediction.

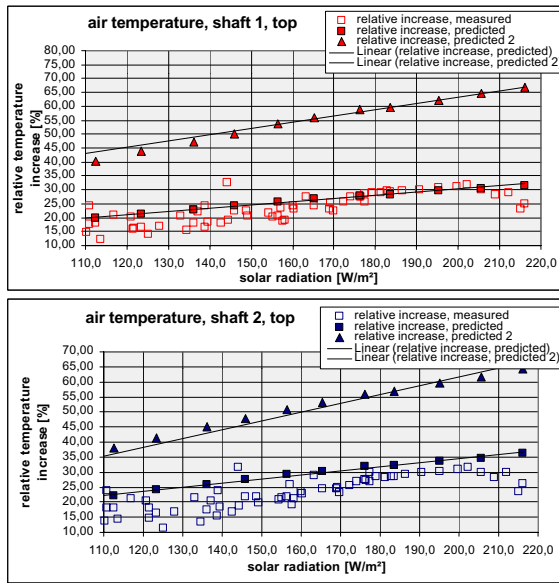


Fig. (M1): Measurement1, difference of results of prediction compared against measurement for using flange/diffuser ("prediction") or orifices ("prediction 2") for the inlet and outlet.

The set up for Measurement 2 was changed so that the shading device was positioned closer to the inner pane (depth of shaft 2: 0.07 m) and the façade inlet and outlet were increased to 0.17 m each. Figure (M2) shows the result of the prediction. Neither prediction is perfect but this time the best results were achieved by modelling orifices instead of flange/diffusers.

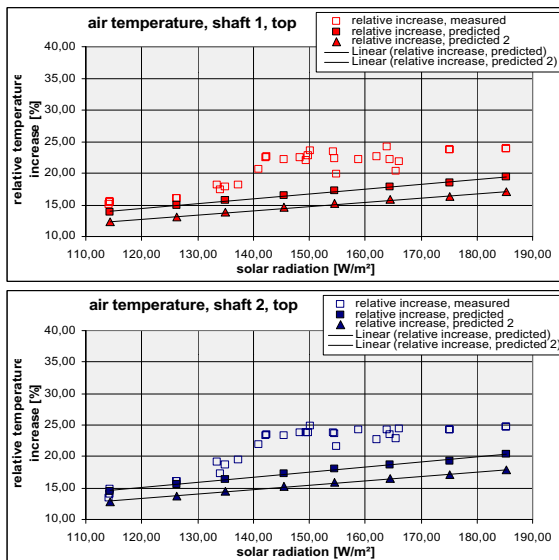


Fig. (M2): Measurement2, difference of results of prediction compared against measurement for using orifices ("prediction") or flange/diffuser ("prediction 2") for the inlet and outlet.

## CONCLUSION

These examples demonstrate the sensitivity of the prediction of, and the difficulty of modelling, flow resistances. There are many factors involved but the main problem is caused by assuming the same flow conditions for natural as those used for mechanical ventilation (using values from mechanical engineering tables). These values have been developed in the past for velocity profiles as they occur in pipes: symmetric and having the highest velocity at the centre (see figure (C1)).

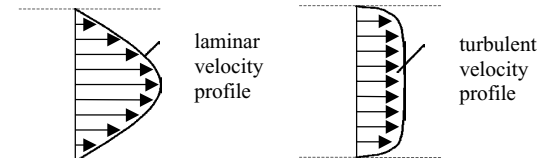


Fig. (C1): Velocity profile for laminar and turbulent flow (pipe, mechanically ventilated).

With natural ventilation however, the driving force is the reduction of the density due to the increase of air temperature. This increase is greater near the heat sources, thus near the panes and the shading device. Further on it might be non-symmetric because of different magnitudes of the heat sources. A laminar profile might look like the one shown in figure (C2).

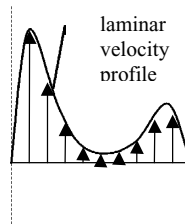


Fig. (C2): Possible laminar velocity profile for natural ventilation

It is obvious, that the flow resistance caused by local changes of geometry is unlikely to have the same magnitude for a symmetric and an almost reversed, non-symmetric velocity profile.

In many cases however, the flow conditions in a double façade will be turbulent as well. With increasing turbulence the velocity profile becomes more similar to the turbulent profile of the pipe flow. This might lead to a better prediction since the resistance factors  $\zeta$  are usually determined under turbulent conditions.

As mentioned previously, along with the air temperature the air velocity was measured as well. The velocity measurement was not sensitive to the flow direction. The prediction algorithm however, calculates the vertical net mass flow. Consequently, the ratio of measured and predicted air velocity can be regarded as an index for the turbulence: the higher the index the more turbulent is the flow (see figure (C3)).

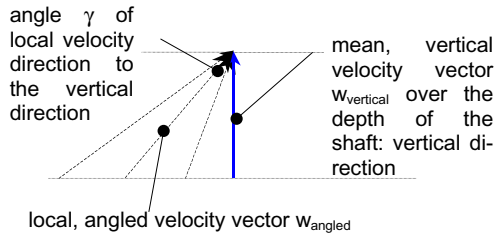


Fig. (C3): Illustration of the ratio of measured and predicted velocity

Such an analysis may lead to the result, that with turbulent flow the accuracy of the prediction increases. Nevertheless, when using the resistance factor  $\zeta$  for analysing the flow characteristics of buoyancy driven ventilation one runs the risk of ending up with wrong results.

## NOMENCLATURE

Expressions:

A	area, [m <sup>2</sup> ]
<b>A</b>	Coefficient matrix, temperature
b	breadth of rectangular shaft, [m]
c	specific heat capacity, [Ws/kg/K]
C	modified Stefan-Boltzmann constant, [W/m <sup>2</sup> /K <sup>4</sup> ]
d	depth of shaft/ height of vents, [m]
e	energy, [W/kg]
g	acceleration due to gravity, [m/s <sup>2</sup> ]
H	domain height, height of the system, [m]
h	heat transfer coefficient, [W/m <sup>2</sup> /K]
$\Sigma h$	sum of heat transfer coefficients, [W/m <sup>2</sup> /K]
k	conductivity, [W/m/K]
$\hat{m}$	mass flow density, [kg/s/m <sup>2</sup> ]
$\dot{m}$	mass flow, [kg/s]
p	pressure, [MPa], [Pa]
$\tilde{q}$	productivity of internal heat source, [W/m <sup>3</sup> ]
$\hat{q}$	rate of energy flow per unit area, [W/m <sup>2</sup> ]
R <sub>air</sub>	gas constant of air, [Ws/kg/K]
T	temperature, [K],[°C]
<b>T</b>	Temperature vector
w	velocity, [m/s]
<b>w</b>	velocity vector
W	weight of the air column, [kg]
<b>x</b>	Eigenvector
$\alpha$	absorption coefficient, absorptivity
$\lambda$	Eigenvalue
$\rho$	density, [kg/m <sup>3</sup> ]
$\zeta$	loss factor

Indices:

c	convection	m	mean value over height
r	radiation		
y	y-direction	i-j	between point i and j
EX	external		
IN	internal	diss	dissipated
IP	inner pane	eff	effective
OP	outer pane		
SD	shading device		
S	shaft		

## ACKNOWLEDGEMENT

The author is particularly grateful to Prof. Michael Lange, University of Hannover, for his support for this paper.

## REFERENCES

- "AIVC Guide to Ventilation", Air Infiltration and Ventilation Centre, Coventry, 1996
- "CIBSE Guide A3, Thermal properties of building structures", Chartered Institution of Building Services Engineers, London 1999
- "CIBSE Guide C4", Chartered Institution of Building Services Engineers, London 1977
- Awbi, H.B., "Ventilation of Buildings", E & FN Spon, London, 1998
- Elsner/Dittman, "Grundlagen der Technischen Thermodynamik, Band 1 Energielehre und Stoffverhalten", 8<sup>th</sup> Edition, Akademie Verlag, Berlin 1992/93
- Elsner/Fischer/Huhn, "Grundlagen der Technischen Thermodynamik, Band 2 Wärmeübertragung", 8<sup>th</sup> Edition, Akademie Verlag, Berlin 1993
- Gertis, Karl, "Der thermische Auftrieb in vertikalen Kanälen und Schächten mit Wärmezufuhr", Institut für Technische Physik Stuttgart, Stuttgart 19??
- Gertis, Karl, "Die Strömungsverhältnisse in Kanälen von Außenwänden", Institut für Technische Physik Stuttgart, Stuttgart 19??
- Gertis, Karl, "Die Temperaturverhältnisse in Kanälen von Bauteilen", Institut für Technische Physik Stuttgart, Stuttgart 19??
- Grigull, Ullrich, "Technische Thermodynamik", 3<sup>rd</sup> Edition, de Gruyter, Berlin/New York 1977
- Kreyszig, Erwin, "Advanced Engineering Mathematics", John Wiley & Sons, Inc., New York 1999
- Li/Lam, "Principles of Fluid Dynamics", Addison-Wesley, London 1964